Quest for novel fluorogenic xanthene dyes: Synthesis, spectral properties and stability of 3-imino-3H-xanthen-6-amine (pyronin) and its silicon analog

Anthony Romieu, Garance Dejouy, Ibai Valverde

Graphical Abstract

To create your abstract, type over the instructions in the template box below.
Fonts or abstract dimensions should not be changed or altered.

Quest for novel fluorogenic xanthene dyes: synthesis, spectral properties and stability of 3-imino-3*H*-xanthen-6-amine (pyronin) and its silicon analog

Leave this area blank for abstract info.

Anthony Romieu*, Garance Dejouy, Ibai E. Valverde

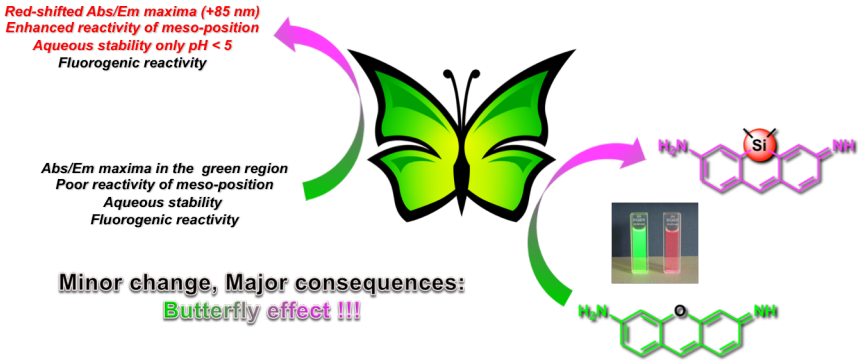

Tetrahedron Letters
journal homepage: www.elsevier.com

Quest for novel fluorogenic xanthene dyes: synthesis, spectral properties and stability of 3-imino-3*H*-xanthen-6-amine (pyronin) and its silicon analog

Anthony Romieu[a,b,*], Garance Dejouy[a], Ibai E. Valverde[a]

[a]*ICMUB, UMR 6302, CNRS, Univ. Bourgogne Franche-Comté, 9, Avenue Alain Savary, 21078 Dijon cedex, France*
[b]*Institut Universitaire de France, 1, Rue Descartes, Bâtiment MONGE, 75231 Paris, France*

ARTICLE INFO

Article history:
Received
Received in revised form
Accepted
Available online

Keywords:
Amino group protection-deprotection
Fluorescent probe
Hetero-xanthene dye
Protease
Pyronin

ABSTRACT

To expand the range of primary aniline fluorophores available and suitable for the design of fluorogenic protease probes, the synthesis of 3-imino-3*H*-xanthen-6-amine (known as pyronin) and its silicon analog (Si-pyronin) was explored and presented here. A comprehensive photophysical study of these two fluorescent anilines, confirms the effectiveness of the heteroatom-substitution approach (O→$SiMe_2$) to yield dramatic red-shifts in absorption and fluorescence maxima of the xanthene scaffold (+85 nm). However, it also revealed its adverse effect on the hydrolytic stability of the Si-pyronin, especially at physiological pH. The pro-fluorescent character and utility of these two fluorogenic (hetero)xanthene dyes are also proved by the preparation and *in vitro* validation of activatable fluorescence "turn-on" probes for penicillin G acylase (PGA).

1. Introduction

Fluorescent organic dyes bearing one or two primary aniline moieties are now recognized as being essential chemical tools for the design of analyte-responsive fluorescent probes applied to sensing/imaging applications.[1,2] Indeed, the protection-deprotection of an optically tunable amino group is often an easy-to-implement method that produces optimal fluorescence "OFF-ON" response and thus high sensitivity for the detection of a target analyte (*i.e.*, enzyme) in complex media (Fig. 1)[3]. The vast majority of fluorogenic anilines currently available are based on benzo[*a*]phenoxazine, coumarin, *N*-alkyl 1,8-naphthalimide and xanthene scaffolds. Well-known examples are oxazine 9 (cresyl violet analog)[4], coumarin 120 (*i.e.*, 7-amino-4-methylcoumarin)[5], *N*-butyl-4-amino-1,8-naphthalimide[6] and rhodamine 110[2] or its disulfonated analog Alexa Fluor® 488[7] (Fig. 1).

Recently, research efforts have been focused on the development and practical applications of alternative aniline-based fluorophores[8], with higher performances in terms of water solubility, cell permeability, (bio)conjugation ability (for further functionalization) and/or spectral properties (especially, high brightness and optimum excitation/emission wavelengths to minimize spectral interferences inherent to sample/medium to be analyzed). Among the various fluorogenic core structures explored, great attention has been paid to rhodamine 110 analogs for which the size of π-conjugated system was expanded or the bridging oxygen atom was replaced by a group 14 element (*i.e.*, C, Si or Ge)[9,10-13]. Less common hybrid structures having a dimethine bridge between an aniline and a second chromophore unit, have also been explored to rapidly access to near-infrared (NIR) fluorogenic dyes for more challenging biosensing/bioimaging applications, especially *in vivo*[14-17] (Fig. 1).

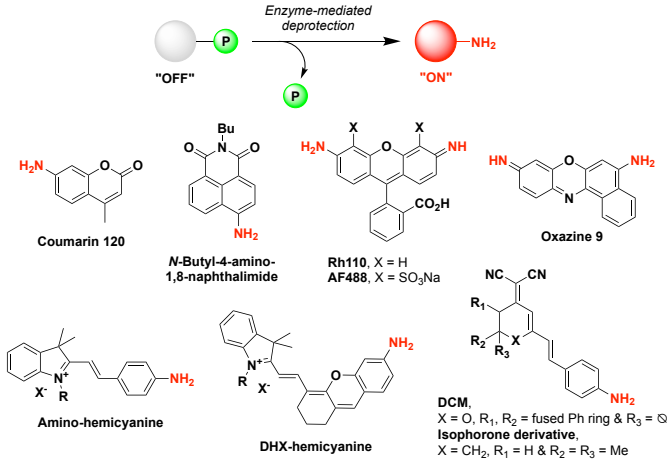

Figure 1. (Top) Principle of the amino group protection-deprotection strategy applied to "OFF-ON" fluorogenic detection of enzyme activity; (middle) structures of fluorescent anilines used in the design of conventional fluorogenic enzyme substrates (Rh110 = rhodamine 110, AF488 = Alexa Fluor® 488); (bottom) aniline-based fluorophores specifically developed for biosensing/bioimaging applications in living cells or *in vivo* (DHX = dihydroxanthene, DCM = dicyanomethylene-4*H*-pyran chromophore).

* Corresponding author. Tel.: +33-3-80-39-36-24; e-mail: anthony.romieu@u-bourgogne.fr.

Surprisingly, none of these studies concerned the most structurally simple xanthene dyes known: pyronins and succineins whereas these diphenylmethane derivatives exhibit remarkable optical properties in the green-yellow spectral range.[18] Despite the reactivity of their *meso*-position towards nucleophiles, that may be problematic for some applications in complex biological media, there is a renewed interest for this class of fluorescent anilines. Indeed, the amino-group protection-deprotection strategy can be easily applied to give valuable activatable (or "smart") fluorescent probes. Furthermore, *in situ* formation of the electronic push-pull conjugated backbone of pyronin dyes, from a non-fluorophore caged precursor and *via* a cascade reaction triggered by the analyte to be detected, has been recently demonstrated by the Yang group and us. This enabled the emergence of "covalent-assembly" type probes whose potential utility and superior performances in terms of detection sensitivity were highlighted through the sensing of several analytes including Sarin nerve agent mimics[19], Hg(II) cations[20] and amidases/proteases (*i.e.*, penicillin G acylase (PGA) and leucine aminopeptidase (LAP))[21].

In this context, we strongly believe that the chemistry of 3-imino-3*H*-xanthen-6-amine **1** (Fig. 2), the only fluorogenic pyronin known to date[22], is worthwhile exploring to identify novel aniline-based fluorophores with valuable properties. We have thus revisited the synthesis of **1** and here we report for the first time its spectroscopic and photophysical characterizations. The preparation and spectral features of its silicon analog (Si-pyronin **2**) are also described for the first time.[23,24] The ability of these two anilines to act as effective optical reporters in fluorogenic enzyme substrates has been finally assessed through the preparation and *in vitro* validation of PGA-activated fluorescent probes.

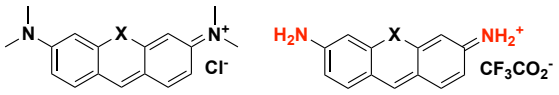

PY, pyronin Y, X = O
TMDHS, X = $SiMe_2$

1, pyronin, X = O
2, Si-pyronin, X = $SiMe_2$

Figure 2. Structures of already known (hetero)pyronins and fluorogenic analogs studied in this work.

Results and discussion

*Synthesis of pyronin **1** and its silicon analog **2***

To date, the synthesis of 3-imino-3*H*-xanthen-6-amine **1**, through a conventional acid-catalyzed condensation between two molecules of 3-aminophenol and formaldehyde followed by spontaneous aromatization, has been described in only one publication written in German[22] (Scheme 1). The work-up of the reaction mixture was not trivial, time-consuming and involved liquid-liquid extractions with butanol, two size-exclusion chromatography over a Sephadex LH-20 column and a counter-ion exchange process to obtain **1** as a perchlorate salt. Furthermore, the sole reported characterization data was curiously a UV-vis absorption spectrum recorded in phosphate buffer (PB, 10 mM, pH 7.0).

In this context, we revisited the purification protocol of this polar fluorophore with a view both to simplify it and to rapidly obtain a highly pure sample for spectroscopic characterization and photophysical studies. Butanol was replaced by the more conventional and less expensive solvent mixture $CHCl_3$-iPrOH (3:1, v/v)[25], and the crude pyronin was easily purified by semi-preparative RP-HPLC using a conventional liquid mobile phase (*i.e.*, step gradient of CH_3CN in aq. TFA 0.1%, pH 1.9). From 1.11 g of cheap starting material 3-aminophenol, it was possible to recover 80 mg of **1** after only two independent HPLC purification runs (overall duration per run = 60 min). This aniline-based fluorophore was fully characterized by IR, ^1H, ^{13}C and ^{19}F NMR and ESI mass spectrometry (see Figs. S4-S9) and all these spectroscopic data were in agreement with the structure assigned. Its high purity (>95%) was confirmed by RP-HPLC analysis and the mass percentage of TFA (31%, ca. 1 TFA per molecule of fluorophore) in freeze-dried sample was determined by ion chromatography.[26]

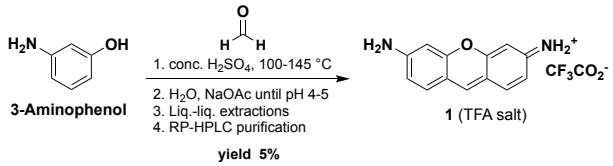

3-Aminophenol

1 (TFA salt)

Scheme 1. Synthesis of fluorogenic pyronin **1** (purification protocol revisited).

The synthetic route devised to obtain silicon analog of 3-imino-3*H*-xanthen-6-amine (Si-pyronin **2**) through the formal substitution O→$SiMe_2$ in the pyronin core structure is depicted in Scheme 2. The key step in the preparation of Si-xanthene dyes (*e.g.*, **TMDHS** and silicon analogs of some pyronin/rosamine derivatives) is the silylation/cyclization process involving the dilithium reagent generated from **4** by halogen-metal exchange and $SiMe_2Cl_2$.[12,24,27,28] Contrary to silicon-containing dyes previously published, the lack of alkyl substituents in both amino groups necessarily implies the temporary protection of primary anilines. By analogy with the synthetic routes towards silicon-fluorescein and sulfone-rosamine, respectively published by the Hanaoka group[29] and us[26], the allyl moiety was used as protecting group (both to remove NH "acidic" protons and to enhance solubility of intermediates in organic solvents) that is stable under a variety of conditions (especially in the presence of RLi/ArLi) and easily removed by Pd(0)-catalysis under mild and neutral conditions.

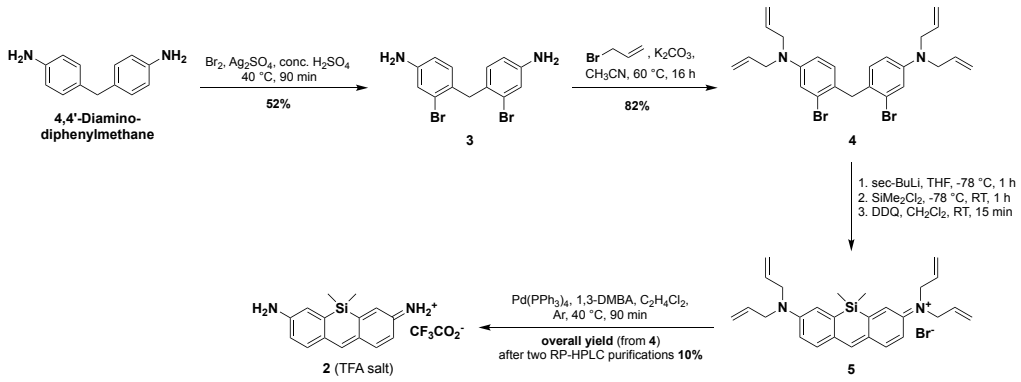

4,4'-Diamino-diphenylmethane

3

4

2 (TFA salt)

5

Scheme 2. Synthesis of fluorogenic Si-pyronin **2** (DDQ = 2,3-dichloro-5,6-dicyano-1,4-benzoquinone, 1,3-DMBA = 1,3-dimethylbarbituric acid).

Thus, the preparation of Si-pyronin **2** began with *meta*-bis-bromination of 4,4'-diaminodiphenylmethane. This S_EAr reaction was performed using bromine and Ag_2SO_4 in concentrated H_2SO_4 at 40 °C for 1 h[30], and purification by automated flash-column chromatography over 25 µm silica gel was effective to perform challenging separation between **3** and its undesired regioisomers. *N*,*N*′-Tetraalkylation of **3** was achieved with an excess of allyl bromide (5.1 equiv.) and anhydrous K_2CO_3 (4 equiv.) in dry CH_3CN at 60 °C. Purification by conventional column chromatography over silica gel provided the key synthetic intermediate **4** in a good 82% yield. Next, halogen-metal exchange reaction with sec-BuLi (2.5 equiv.) in dry THF à -78 °C, generated the 2,2'-methylenebis(aryllithium) species, on which the subsequent reaction with $SiMe_2Cl_2$ (1.8 equiv.) and finally DDQ-mediated oxidation in CH_2Cl_2, afforded the blue-colored *N*,*N*,*N*′,*N*′-tetraallyl-Si-pyronin **5**. Our first attempts to isolate this dye in a pure form by column chromatography over silica gel failed because a disproportionation reaction was occurred in the presence of air to give a mixture of **5** and its reduced and keto forms (Figs. S24 and S25). Consequently, it became more relevant to do only washings with aq. $NaHCO_3$ in order to remove reduced hydroquinone form of DDQ and to subject directly the crude **5** to Tsuji-Trost deallylation conditions. Thus, this final deprotection step was readily achieved by treatment with a cat. amount of $Pd(PPh_3)_4$ and a large excess of 1,3-dimethylbarbituric acid (4.4 equiv) in degassed $C_2H_4Cl_2$ at 40 °C. Purification by semi-preparative HPLC afforded pure Si-pyronin **2** as a TFA salt (mass percentage of TFA in freeze-dried sample = 33.5%, determined by ion chromatography, ca. 1 TFA per molecule of fluorophore) and in a moderate yet not optimized overall yield (10%) from **4**. The structure was proven by NMR (^1H, ^{13}C, ^{19}F and ^{29}Si) and ESI mass analyses (see Supplementary data and Figs. S26-S33) and the high level of purity (>99% whatever the wavelength used for the UV-vis detection) was confirmed by RP-HPLC-based analytical control (see Supplementary data and Figs. S33 and S34).

*Stability and photophysical characterization of pyronin **1** and its silicon analog **2***

Since the bioanalytical applications envisioned for these fluorogenic dyes generally involve to work under physiological conditions, the photophysical properties of these two compounds were primarily determined in phosphate buffered saline (PBS, 100 mM + 150 mM NaCl, pH 7.4). However, the poor stability of Si-pyronin **2** under these simulated physiological conditions (*vide infra*) pushed us to consider acidic buffers as the aq. solvents for the photophysical characterization of this hetero-xanthene dye (see Table 1 for absorption/emission properties and Fig. 3 for the corresponding spectra).

Table 1. Photophysical properties of fluorophores and PGA-sensitive probes studied in this work, determined at 25 °C.

Cmpd	Solvent	λ_{max} Abs (nm)[a]	λ_{max} Em (nm)	ε (M^{-1} cm^{-1})	Φ_F (%)[b,c]
1	PBS	496	514	81 400	92
TMDHS[d]	H_2O	634	653	64 200	18
2	aq. FA 0.1%[e]	580	597	42 200	89
2	NaOAc	580	597	47 900	89
7	PB	238	-[f]	23 000	-[f]
9	PB	267	-[f]	22 650	-[f]
9	NaOAc	265	-[f]	28 600	-[f]

[a]Further bands with maxima within the UV spectral range are also observed in spectra of **1** (241, 260, 280 and 320 nm) and **2** (290 and 308 nm).
[b]Determined using fluorescein as a standard (Φ_F = 95% in 0.1 M NaOH, Ex at 450 nm) for **1** and SR101 as a standard (Φ_F = 95% in EtOH, Ex at 545 nm) for **2**.[31]
[c]Absolute fluorescence quantum yield was also determined using an integration sphere (45% in PBS for **1** and 56% in CH_3CN for **2**, see Supplementary data for details).
[d]Values determined and reported by Fu *et al.*[27]
[e]0.1% aqueous formic acid (pH 2.5).
[f]Non-fluorescent.

Pyronin **1** exhibits spectral features in the green region, quite similar to popular fluorophores namely fluorescein and Alexa Fluor® 488. The perfect matching between the absorption and excitation spectra (Fig. 3A) confirms the lack of non-fluorescent H-type aggregates in neutral aqueous solutions. This may be credited to the small compact size and hydrophilic character of this xanthene dye. The same photophysical study has been considered with the silicon analog **2** but we found that this compound is unstable in aq. physiological conditions due to the marked electrophilicity of its *meso*-position (*i.e.*, C-9 position of xanthene scaffold) and hence its propensity to undergo nucleophilic attack by a water molecule or a hydroxyde anion. Indeed, despite lower electronegativity of Si atom compared to O atom (1.9 against 3.5 in Linus Pauling's scale), the lack of electron-donating ability through +M effect seems to be critical in this regard. The same poor hydrolytic stability was also evidenced in PB and ultrapure water, by the rapid discoloration of initially pink solutions visible to the naked eye. To establish the pH range at which Si-pyronin **2** is fully stable and thus selecting the appropriate aq. medium for photophysical measurements, its spectral behavior was studied over the pH range 3.5-9.5 through incubation in various buffers (NaOAc, PB and borate, for 15 min at 23 °C) and subsequent absorbance measurement at 580 nm. By drawing a pH-dependent absorption curve (Fig. 4), we were able to determine the pK value of the corresponding hydration equilibrium between Si-pyronin **2** and Si-xanthydrol **6** (pK = 6.5). Furthermore, this curve clearly shows that the hydrolytic stability of **2** is optimal at pH < 5. It is worth stating that pyronin **1** was found to be full-stable within the same pH range (see Supplementary data and Fig. S3), supporting our hypothesis about the electrophilic character of *meso*-position weakened by +M effect of O-10 atom (*vide supra*).

We decided to investigate the photophysical properties of **2** in NaOAc buffer (100 mM, pH 4.8). **2** shows strong and sharp absorption (full-width half maximum, FWHM, $\Delta\lambda_{1/2\ max}$ = 40 nm) and emission bands in the orange-red region of the spectrum (see Fig. 3B). The absorption maximum is centered at 580 nm, with a 85 nm bathochromic shift compared with pyronin **1**. Molar extinction coefficient (ε = 47 900 M^{-1} cm^{-1}) is of the same order of magnitude as that of silicon analog of pyronin Y (**TMDHS**, ε = 64 200 M^{-1} cm^{-1} in water)[27]. The emission band peaked at 595 nm is very narrow (25 nm FWHM) and the value of relative fluorescence quantum yield (Φ_F = 89%) is really impressive and equivalent to that of larger fluorophores exhibiting the same spectral features (*e.g.*, sulforhodamine 101, SR101, MW = 606.7, Abs/Em 575/595 nm, Φ_F = 95% in EtOH). As observed for pyronin **1**, the absorption and excitation spectra are perfectly superimposable (Fig. 3B), suggesting the presence of a single absorbing species in solution, and the lack of equilibrium between Si-xanthene and Si-xanthydrol forms in NaOAc buffer.

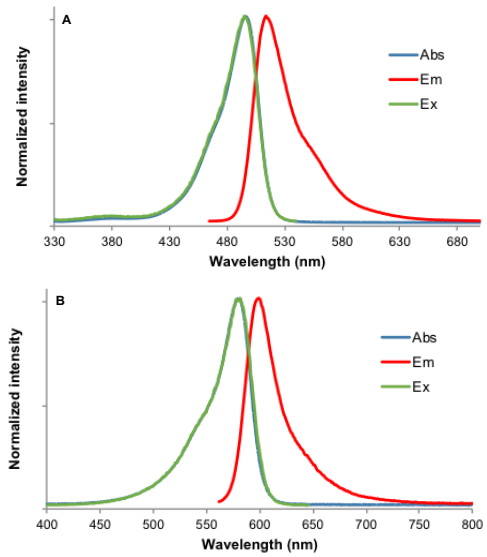

Figure 3. Normalized absorption (blue), excitation (Em 550 or 660 nm, slit 5 nm, green) and emission (Ex 450 or 545 nm, slit 5 nm, red) spectra of pyronin **1** in PBS (pH 7.4) (A) and Si-pyronin **2** in NaOAc buffer (pH 4.8) (B) at 25 °C.

In order to complement our study devoted to these two unusual fluorescent anilines, it was essential to demonstrate their fluorogenic behavior through the reversible masking of their primary amino groups, in the context of fluorescence "turn-on" detection of analytes.

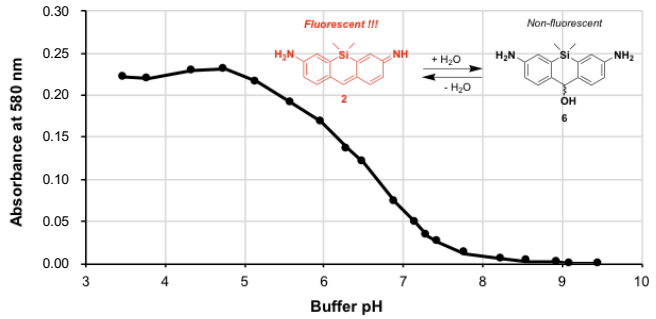

Figure 4. pH-Dependant maximum absorbance (580 nm) curve for Si-pyronin **2** (concentration: 4.5 µM in the corresponding buffer, 15 min of incubation before absorbance measurement).

*Fluorogenic reactivity of pyronin **1** and its silicon analog **2**. Synthesis and in vitro validation of PGA-sensitive probes **7** and **9***

To achieve this goal, we explored the synthesis of two unusual PGA substrates in which the green/orange-red fluorescence of pyronin/Si-pyronin reporter is unveiled through two distinct and sequential events: enzymatic hydrolysis of phenylacetamide moieties and 1,6-elimination process promoted by the released phenylogous amine. PGA (also known as penicillin amidase, EC 3.5.1.11) was chosen as model protease because this hydrolytic enzyme has two clear advantages: (1) a structurally simple substrate (phenylacetamide) than can be easily installed on a wide range of fluorescent anilines through amidification of their primary amino group(s) and (2) a commercial availability at low cost[32].

Bis-amidation of **1** and **2** was achieved by treatment with an excess of phenylacetyl chloride (PhAcCl, 17 equiv.) and DIEA (4-4.5 equiv.) in dry DMF (Schemes 3 and 4). We intentionally used a large excess of acyl chloride in order to promote the introduction of phenylacetoxy (PhAcO-) moiety onto the *meso*-position. Indeed, once complete, the reaction was quenched by adding aq. TFA 1% to produce a significant amount of phenylacetic acid (PhAcOH) that may able to displace chloride or other leaving groups onto the C-9 position of the (hetero)xanthene scaffold. In the case of pyronin **1**, these conditions led to the desired fluorogenic PGA substrate **7** as the major product. After isolation by semi-preparative RP-HPLC, the structure of **7** was confirmed by NMR and ESI mass analyses (see Supplementary data, Figs. S35-S37).

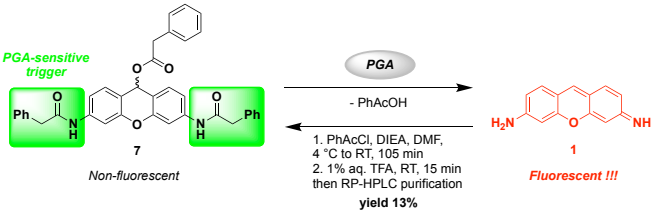

Scheme 3. Synthesis of PGA-sensitive probe **7** and its enzymatic activation.

Conversely, when Si-pyronin **2** was subjected to the same acylation conditions, the expected PGA-sensitive probe **8** was only formed as a minor product. Surprisingly, the major compound isolated by semi-preparative RP-HPLC was identified as the α-phenyl 9-Si-pyronin-acetaldehyde derivative **9** (see Supplementary data for NMR and ESI mass analyses, Figs. S41-S43). The proposed mechanism to explain the conversion of **8** into **9**, *via* a Vilsmeier-type reaction is shown in Scheme 4. Once again, the unexpected reactivity of phenylacetoxy ester **8** in line with its poor stability in aq. buffers (see Supplementary data), can be explained by the fact that the electropositivity of the intracyclic Si atom cannot fully compensate the electrophilicity of the C-9 position.

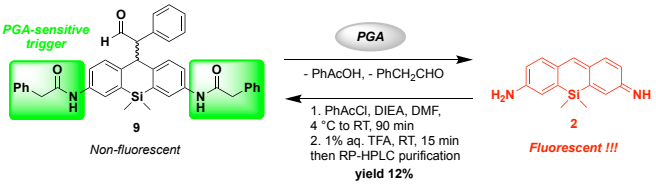

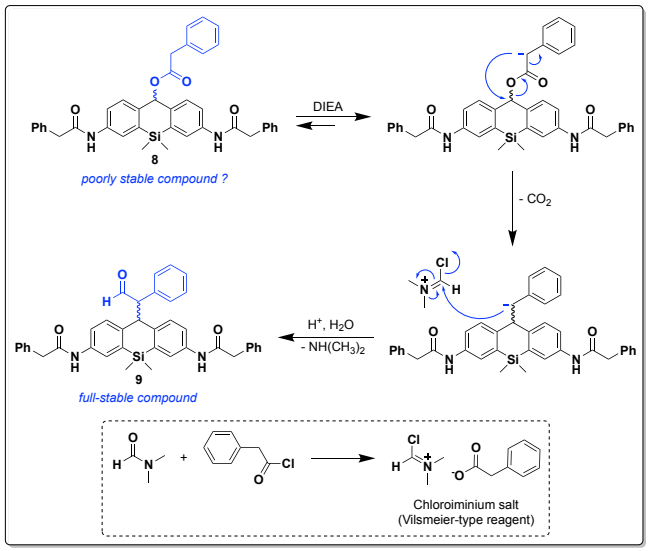

Scheme 4. (Top) Synthesis of PGA-sensitive probe **9** and its enzymatic activation; (bottom) proposed mechanism to explain the conversion of **8** into **9**.

As expected, the two probes **7** and **9** exhibit absorption only in the UV range (220-370 nm, Figs. S40 and S46) and are non-fluorescent in both acetate and phosphate buffers (pH 4.8 and 7.4 respectively). Their sensing response to commercial PGA (from *Escherichia coli*) was studied by time-dependent fluorescence

analyses. The resulting kinetic curves are shown in Fig. 5 for **9** (see Fig. S51 for the curves obtained with **7**). When the enzymatic activation was performed at pH 4.8 (pH where the released Si-pyronin is full-stable but not optimal for stability and activity of PGA), a significant and gradual increase of orange-red fluorescence of Si-pyronin (Ex/Em 580/595 nm) was observed (Fig. 5). A plateau indicating the complete hydrolysis of **9** by PGA and subsequent aromatization of the intermediate through 1,6-elimination process (the rate-limiting step of probe activation) was reached only after a lengthy incubation time (more than 6 h).

However, after 15 h (overnight incubation), a dramatic 2600-fold increase in fluorescence was obtained (Fig. S53). Furthermore, no fluorescence signal changes were observed in the absence of amidase, confirming the full stability of the probe **9** in acetate buffer. Interestingly, the same fluorescence-based *in vitro* assay conducted in PB (pH 7.4) provided a lower but significant "OFF-ON" response (a 9-fold decrease compared to enzyme activation in NaOAc buffer, Fig. S54) whereas Si-pyronin **2** is assumed to be unstable under these simulated physiological conditions. A stabilization/protective effect of the local environment of enzyme in contact with **2** could be advanced to explain this unexpected but positive result. Further experiments are currently in progress to clarify the behavior of fluorescent Si-pyronin **2** in complex biological media. Finally, the presence of Si-pyronin dye **2** in the enzymatic reaction mixtures was unambiguously confirmed by RP-HPLC analyses (fluorescence detection, t_R = 3.5 min) and compared with an authentic sample of synthetic Si-pyronin **2** used as reference (Figs. S56 and S57). The same methodology was used to identify the fluorescent species (pyronin **1**) found in enzymatic reaction mixtures related to activation of probe **7** with PGA (Fig. S55). All these results demonstrate the potential utility of O-/Si-pyronin dyes bearing two primary anilines, as fluorogenic labels in enzyme-activatable molecular probes.

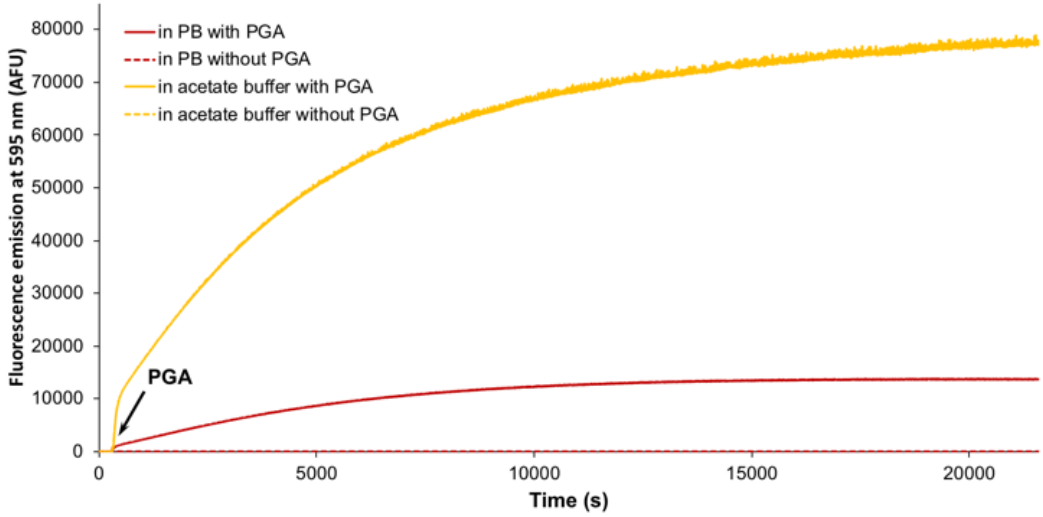

Figure 5. Time-dependent changes in the orange-red fluorescence intensity (Ex/Em 580/595 nm, slit = 5 nm) of fluorogenic probe **9** (concentration: 1 µM) in the presence of PGA (1 U) at 37 °C. *Please note: PGA was added after 5 min of incubation of probe in buffer alone.*

Conclusion

To the best of our knowledge, the present work is the first comprehensive survey devoted to the synthesis and characterizations of the most structurally simple fluorogenic xanthene dyes known to date. These fluorophores namely 3-imino-3*H*-xanthene-6-amine **1** and its silicon analog Si-pyronin **2** exhibit outstanding spectral properties in aq. solution, and dramatic bathochromic shift as a result of the substitution of the pyronin oxygen bridge atom by silicon enables to cover a wide spectral range from green to red (*ca.* 450-650 nm) while keeping a small compact size and a marked hydrophilic character. A study of the hydrolytic stability of Si-pyronin **2** has outlined the pH range (pH < 5) of aq. media wherein this orange-red emitter is actually usable. The availability of two primary anilines within the (hetero)xanthene core structure of these dyes gives them a unique fluorogenic reactivity and to place them high in the list of fluorophores applicable to the design of reaction-based small-molecule probes for analyte sensing/bioimaging. Since the reactivity of the *meso*-position can be finely tuned by the heteroatom-substitution approach (O→$SiMe_2$), the nucleophilic displacement of the C-9 substituent of fluorogenic enzyme substrates related to **8**, may be an entrance gate towards "smart" theranostic drug delivery agents that provide a cytotoxic chemotherapeutic response while facilitating fluorescence imaging of cancer cells[33].

Acknowledgments

This work is supported by the CNRS, Université de Bourgogne and Conseil Régional de Bourgogne through the "Plan d'Actions Régional pour l'Innovation (PARI) and the "Fonds Européen de Développement Régional (FEDER)" programs. G. D. gratefully acknowledges the Burgundy Franche-Comté region for his Ph. D. grant and bioMerieux company (R&D Microbiology) as industrial sponsor. Financial support from Institut Universitaire de France (IUF, 2013-2018), the Burgundy region ("FABER" programme, PARI Action 6, SSTIC 6 "Imagerie, instrumentation, chimie et applications biomédicales") and GDR CNRS "Agents d'Imagerie Moléculaire" (AIM) 2037 are also greatly acknowledged. The authors thank the "Plateforme d'Analyse Chimique et de Synthèse Moléculaire de l'Université de Bourgogne" (PACSMUB, http://www.wpcm.fr) for access to spectroscopy instrumentation. COBRA lab (UMR CNRS 6014) and Iris Biotech company are warmly thanked for the generous gift of some chemical reagents used in this work. The authors also thank Dr. Sylvain Debieu for

preliminary research about fluorogenic pyronin dyes, Dr. Myriam Laly (University of Burgundy, PACSMUB) for the determination of TFA content in samples purified by RP-HPLC, Dr. Ewen Bodio (University of Burgundy, ICMUB, UMR CNRS 6302, OCS team) for access to SAFAS Xenius XC spectrofluorimeter (equipped with an integrating sphere) and Dr. Jean-Franck Bussotti / M. Olivier Chaudon (SAFAS Monaco company) for their precious advice regarding the determination of absolute fluorescence quantum yields.

Supplementary data

Supplementary data (all synthetic procedures, spectroscopic and photophysical characterizations of fluorophores and PGA-sensitive probes, stability studies, *in vitro* fluorescence assays and HPLC-fluorescence analyses described in this work) associated with this article can be found, in the online version:

References and note

1. For selected reviews, see a) X. Chen, M. Sun, H. Ma, Curr. Org. Chem. 10 (2006) 477-489; b) C.R. Drake, D.C. Miller, E.F. Jones, Curr. Org. Synth. 8 (2011) 498-520; c) J. Chan, S.C. Dodani, C.J. Chang, Nat. Chem. 4 (2012) 973-984; d) J.B. Grimm, L.M. Heckman, L.D. Lavis, Prog. Mol. Biol. Transl. Sci. 113 (2013) 1-34; e) W. Chyan, R.T. Raines, ACS Chem. Biol. 13 (2018) 1810-1823; f) H.-W. Liu, L. Chen, C. Xu, Z. Li, H. Zhang, X.-B. Zhang, W. Tan, Chem. Soc. Rev. 47 (2018) 7140-7180; g) K. Singh, A.M. Rotaru, A.A. Beharry, ACS Chem. Biol. 13 (2018) 1785-1798.
2. M. Beija, C.A.M. Afonso, J.M.G. Martinho, Chem. Soc. Rev. 38 (2009) 2410-2433.
3. Y. Tang, D. Lee, J. Wang, G. Li, J. Yu, W. Lin, J. Yoon, Chem. Soc. Rev. 44 (2015) 5003-5015.
4. For selected examples, see: a) C.J.F. Van Noorden, E. Boonacker, E.R. Bissell, A.J. Meijer, J. van Marle, R.E. Smith, Anal. Biochem. 252 (1997) 71-77; b) Y. Hu, H. Li, W. Shi, H. Ma, Anal. Chem. 89 (2017) 11107-11112.
5. J.K.P. Weder, K.-P. Kaiser, J. Chromatogr. A 698 (1995) 181-201.
6. For selected examples, see: a) W.C. Silvers, B. Prasai, D.H. Burk, M.L. Brown, R.L. McCarley, J. Am. Chem. Soc. 135 (2013) 309-314; b) S.U. Hettiarachchi, B. Prasai, R.L. McCarley, J. Am. Chem. Soc. 136 (2014) 7575-7578; c) Q. Jin, L. Feng, D.-D. Wang, Z.-R. Dai, P. Wang, L.-W. Zou, Z.-H. Liu, J.-Y. Wang, Y. Yu, G.-B. Ge, J.-N. Cui, L. Yang, ACS Appl. Mater. Interfaces 7 (2015) 28474-28481; d) X. Chen, X. Ma, Y. Zhang, G. Gao, J. Liu, X. Zhang, M. Wang, S. Hou, Anal. Chim. Acta 1033 (2018) 193-198.
7. a) F. Mao, W.-Y. Leung, R.P. Haugland WO Patent 9915517, 1999; b) N. Panchuk-Voloshina, R.P. Haugland, J. Bishop-Stewart, M.K. Bhalgat, P.J. Millard, F. Mao, W.-Y. Leung, R.P. Haugland, J. Histochem. Cytochem. 47 (1999) 1179-1188; c) J.E. Berlier, A. Rothe, G. Buller, J. Bradford, D.R. Gray, B.J. Filanoski, W.G. Telford, S. Yue, J. Liu, C.-Y. Cheung, W. Chang, J.D. Hirsch, J.M. Beechem, R.P. Haugland, R.P. Haugland, J. Histochem. Cytochem. 51 (2003) 1699-1712.
8. For unsymmetrical analogs of sulforhodamine 101 bearing a primary aniline, see: a) A. Chevalier, P.-Y. Renard, A. Romieu, Chem. - Eur. J. 20 (2014) 8330-8337; b) A. Chevalier, W. Piao, K. Hanaoka, T. Nagano, P.-Y. Renard, A. Romieu, Methods Appl. Fluoresc. 3 (2015) 044004.
9. For the first example of fluorogenic carbopyronin, see: J.B. Grimm, A.J. Sung, W.R. Legant, P. Hulamm, S.M. Matlosz, E. Betzig, L.D. Lavis, ACS Chem. Biol. 8 (2013) 1303-1310.
10. For the first synthesis of carborhodamine dyes, see: K. Kolmakov, V.N. Belov, C.A. Wurm, B. Harke, M. Leutenegger, C. Eggeling, S.W. Hell, Eur. J. Org. Chem. (2010) 3593-3610.
11. For reviews about Si-xanthene dyes and related probes, see: a) Y. Kushida, T. Nagano, K. Hanaoka, Analyst 140 (2015) 685-695; b) T. Ikeno, T. Nagano, K. Hanaoka, Chem. - Asian J. 12 (2017) 1435-1446.
12. Y. Koide, Y. Urano, K. Hanaoka, T. Terai, T. Nagano, ACS Chem. Biol. 6 (2011) 600-608.
13. For selected examples of Si-rosamines, see: a) Y. Kushida, K. Hanaoka, T. Komatsu, T. Terai, T. Ueno, K. Yoshida, M. Uchiyama, T. Nagano, Bioorg. Med. Chem. Lett. 22 (2012) 3908-3911; b) W. Piao, S. Tsuda, Y. Tanaka, S. Maeda, F. Liu, S. Takahashi, Y. Kushida, T. Komatsu, T. Ueno, T. Terai, T. Nakazawa, M. Uchiyama, K. Morokuma, T. Nagano, K. Hanaoka, Angew. Chem., Int. Ed. 52 (2013) 13028-13032; c) N. Shin, K. Hanaoka, W. Piao, T. Miyakawa, T. Fujisawa, S. Takeuchi, S. Takahashi, T. Komatsu, T. Ueno, T. Terai, T. Tahara, M. Tanokura, T. Nagano, Y. Urano, ACS Chem. Biol. 12 (2017) 558-563.
14. For examples of probes based on amino-hemicyanine dye, see: a) F. Kong, Y. Zhao, Z. Liang, X. Liu, X. Pan, D. Luan, K. Xu, B. Tang, Anal. Chem. 89 (2017) 688-693; b) M. Hu, C. Yang, Y. Luo, F. Chen, F. Yang, S. Yang, H. Chen, Z. Cheng, K. Li, Y. Xie, J. Mater. Chem. B 6 (2018) 2413-2416.
15. For examples of probes based on DHX-hemicyanine hybrids, see: a) X. Xie, X.e. Yang, T. Wu, Y. Li, M. Li, Q. Tan, X. Wang, B. Tang, Anal. Chem. 88 (2016) 8019-8025; b) X. He, Y. Hu, W. Shi, X. Li, H. Ma, Chem. Commun. 53 (2017) 9438-9441; c) L. Li, W. Shi, X. Wu, X. Li, H. Ma, Anal. Bioanal. Chem. 410 (2018) 6771-6777; d) J. Xing, Q. Gong, R. Zou, Z. Li, Y. Xia, Z. Yu, Y. Ye, L. Xiang, A. Wu, J. Mater. Chem. B 6 (2018) 1449-1451.
16. For examples of probes based on DCM scaffold, see: a) W. Sun, J. Fan, C. Hu, J. Cao, H. Zhang, X. Xiong, J. Wang, S. Cui, S. Sun, X. Peng, Chem. Commun. 49 (2013) 3890-3892; b) Y. Zheng, M. Zhao, Q. Qiao, H. Liu, H. Lang, Z. Xu, Dyes Pigm. 98 (2013) 367-371; c) J. Fan, W. Sun, Z. Wang, X. Peng, Y. Li, J. Cao, Chem. Commun. 50 (2014) 9573-9576; d) X. Wu, X. Sun, Z. Guo, J. Tang, Y. Shen, T.D. James, H. Tian, W. Zhu, J. Am. Chem. Soc. 136 (2014) 3579-3588; e) D. Yu, F. Huang, S. Ding, G. Feng, Anal. Chem. 86 (2014) 8835-8841; f) S. Cao, Z. Pei, Y. Xu, Y. Pei, Chem. Mater. 28 (2016) 4501-4506; g) K. Gu, Y. Liu, Z. Guo, C. Lian, C. Yan, P. Shi, H. Tian, W.-H. Zhu, ACS Appl. Mater. Interfaces 8 (2016) 26622-26629; h) L. Cui, Y. Shi, S. Zhang, L. Yan, H. Zhang, Z. Tian, Y. Gu, T. Guo, J. Huang, Dyes Pigm. 139 (2017) 587-592; i) W. Feng, M. Li, Y. Sun, G. Feng, Anal. Chem. 89 (2017) 6106-6112; j) Y. Kong, J. Smith, K. Li, J. Cui, J. Han, S. Hou, M.L. Brown, Bioorg. Med. Chem. 25 (2017) 2226-2233; k) P. Liu, B. Li, C. Zhan, F. Zeng, S. Wu, J. Mater. Chem. B 5 (2017) 7538-7546; l) Y. Liu, S. Zhu, K. Gu, Z. Guo, X. Huang, M. Wang, H.M. Amin, W. Zhu, P. Shi, ACS Appl. Mater. Interfaces 9 (2017) 29496-29504; m) R.R. Nawimanage, B. Prasai, S.U. Hettiarachchi, R.L. McCarley, Anal. Chem. 89 (2017) 6886-6892; n) L.J. O'Connor, I.N. Mistry, S.L. Collins, L.K. Folkes, G. Brown, S.J. Conway, E.M. Hammond, ACS Cent. Sci. 3 (2017) 20-30; o) Z. Wang, H. Wu, P. Liu, F. Zeng, S. Wu, Biomaterials 139 (2017) 139-150.
17. For examples of probes based on isophorone scaffold, see: a) T. Liu, J. Lin, Z. Li, L. Lin, Y. Shen, H. Zhu, Y. Qian, Analyst 140 (2015) 7165-7169; b) K. Xiang, Y. Liu, C. Li, B. Tian, T. Tong, J. Zhang, Dyes Pigm. 123 (2015) 78-84; c) K. Xiang, Y. Liu, C. Li, B. Tian, J. Zhang, RSC Adv. 5 (2015) 52516-52521; d) W. Zhang, F. Liu, C. Zhang, J.-G. Luo, J. Luo, W. Yu, L. Kong, Anal. Chem. 89 (2017) 12319-12326; e) T. Liu, J. Ning, B. Wang, B. Dong, S. Li, X. Tian, Z. Yu, Y. Peng, C. Wang, X. Zhao, X. Huo, C. Sun, J. Cui, L. Feng, X. Ma, Anal. Chem. 90 (2018) 3965-3973.
18. a) F.H. Kasten, Stain Technol. 37 (1962) 265-275; b) P. Wright, U.b. Staff In; John Wiley & Sons, Inc, 2014.
19. Z. Lei, Y. Yang, J. Am. Chem. Soc. 136 (2014) 6594-6597.
20. L. Song, Z. Lei, B. Zhang, Z. Xu, Z. Li, Y. Yang, Anal. Methods 6 (2014) 7597-7600.
21. a) S. Debieu, A. Romieu, Org. Biomol. Chem. 15 (2017) 2575-2584; b) S. Debieu, A. Romieu, Tetrahedron Lett. 59 (2018) 1940-1944.
22. W. Müller, Justus Liebigs Ann. Chem. (1974) 334-335.
23. Si-pyronin **2** is claimed in a patent but never synthesized: Y. Urano, M. Kamiya, A. Morozumi, S. Uno, K. Umezawa WO Patent 2016136328, 2016.
24. For recent examples of unsymmetrical Si-rosamines bearing a primary aniline, see: a) K. Hanaoka, Y. Kagami, W. Piao, T. Myochin, K. Numasawa, Y. Kuriki, T. Ikeno, T. Ueno, T. Komatsu, T. Terai, T. Nagano, Y. Urano, Chem. Commun. 54 (2018) 6939-6942; b) R.J. Iwatate, M. Kamiya, K. Umezawa, H. Kashima, M. Nakadate, R. Kojima, Y. Urano, Bioconjugate Chem. 29 (2018) 241-244.
25. I.E. Valverde, A.F. Delmas, V. Aucagne, Tetrahedron 65 (2009) 7597-7602.
26. G. Dejouy, M. Laly, I.E. Valverde, A. Romieu, Dyes Pigm. 159 (2018) 262-274.
27. M. Fu, Y. Xiao, X. Qian, D. Zhao, Y. Xu, Chem. Commun. (2008) 1780-1782.

28. a) T. Pastierik, P. Šebej, J. Medalová, P. Štacko, P. Klán, J. Org. Chem. 79 (2014) 3374-3382; b) H. Nie, L. Qiao, W. Yang, B. Guo, F. Xin, J. Jing, X. Zhang, J. Mater. Chem. B 4 (2016) 4826-4831; c) H. Zhang, J. Liu, L. Wang, M. Sun, X. Yan, J. Wang, J.-P. Guo, W. Guo, Biomaterials 158 (2018) 10-22; d) M. Du, B. Huo, J. Liu, M. Li, A. Shen, X. Bai, Y. Lai, L. Fang, Y. Yang, J. Mater. Chem. C 6 (2018) 10472-10479.
29. T. Egawa, Y. Koide, K. Hanaoka, T. Komatsu, T. Terai, T. Nagano, Chem. Commun. 47 (2011) 4162-4164.
30. J.H. Gorvin, J. Chem. Soc. (1955) 83-89.
31. A.M. Brouwer, Pure Appl. Chem. 83 (2011) 2213-2228.
32. For instance, only 100 euros for 1000 units, see https://www.iris-biotech.de/de/ez50150.
33. For reviews, see: a) R. Kumar, W.S. Shin, K. Sunwoo, W.Y. Kim, S. Koo, S. Bhuniya, J.S. Kim, Chem. Soc. Rev. 44 (2015) 6670-6683; b) M.H. Lee, A. Sharma, M.J. Chang, J. Lee, S. Son, J.L. Sessler, C. Kang, J.S. Kim, Chem. Soc. Rev. 47 (2018) 28-52.